# Electronic and thermoelectric properties of $CuCoO_2$: Density functional calculations

D. J. Singh
*Materials Science and Technology Division, Oak Ridge National Laboratory, Oak Ridge, Tennessee 37831-6032, USA*
(Received 26 May 2007; revised manuscript received 17 July 2007; published 8 August 2007)

Density functional calculations are used to elucidate the electronic structure and some transport properties of $CuCoO_2$. We find an electronic structure with similarities to $Na_xCoO_2$, although it is much less two dimensional. In particular, there are narrow manifolds of $t_{2g}$ and $e_g$ states. Application of Boltzmann transport theory to the calculated band structure shows high thermopowers comparable to $Na_xCoO_2$ for both *p*- and *n*-type doping.

DOI: 10.1103/PhysRevB.76.085110 PACS number(s): 72.15.Jf, 71.20.−b, 74.25.Fy, 73.50.Jt

$Na_xCoO_2$ and some closely related misfit cobaltate compounds constitute the presently known high figure of merit[1] (*ZT*) oxide thermoelectrics suitable for power generation at temperatures characteristic of waste heat.[2–6] These materials are based on triangular sheets of octahedrally coordinated Co and are invariably *p* type. The transport properties generally reflect the layered crystal structure in that they are highly two dimensional; the high thermoelectric figure of merit exists for transport along the layers, with much lower performance for perpendicular transport.[3] This complicates practical applications since either single crystals or a highly oriented material is needed. In addition, in order to develop all oxide thermoelectric devices, an *n*-type oxide material with comparable *ZT* needs to be found for the *n*-type legs.

The essential ingredient in the high *ZT* of $Na_xCoO_2$ is the existence of a high thermopower $S \sim 100\ \mu V/K$ at 300 K increasing to $\sim 200\ \mu V/K$ at a high temperature, even though the material has a high metallic carrier density of $\sim 0.3$ holes per Co. This is remarkable because, in general, materials with comparable values of *S* are doped semiconductors with much lower carrier concentrations. This unusual thermoelectric behavior has been explained in two ways: a many body approach which yields a high temperature limiting value of *S* and relies on strong correlations and the particular electronic configuration of Co to produce a high thermopower[7] and a conventional Boltzmann transport approach for metals[8,9] applied to the local density approximation band structure of $Na_xCoO_2$,[10–12] as may be done for ordinary thermoelectrics.[13] Within this approach, the essential ingredient in the thermopower is the position of the Fermi energy near the top of a very narrow set of bands of a Co $t_{2g}$ character. In spite of the fact that both these bands and the higher lying $e_g$ bands are very flat, the Co *d* orbitals hybridize strongly with *p* states from the neighboring O ions. This happens because of the topology of the Co-O sheets, which have nearly 90° Co-O-Co bond angles. Considering that the essential ingredient is the presence of narrow *d* electron bands and that this is related to structural features, it is perhaps not surprising that similarly high thermopowers are also predicted for *n*-type doping into the $e_g$ bands and for related rhodates. However, both $Na_xCoO_2$ and the related rhodates have anomalously large crystal field gaps, in excess of 1 eV, between the $t_{2g}$ and $e_g$ manifolds, again reflecting the combination of narrow bands and strong hybridization.[14] Therefore, it may be very difficult to dope these compounds *n*-type with mobile electrons to realize the high thermopowers that are predicted if this can be done. As such, it is of interest to examine other compounds with related bonding topologies in order to find other candidate oxide thermoelectrics with properties complementary to those of $Na_xCoO_2$. The purpose of this study is to examine one promising candidate, specifically $CuCoO_2$.

$CuCoO_2$ occurs in a rhombohedral structure,[15] space group $R\bar{3}m$ (166), related to a series of other Cu–transition element oxides with a similar structure.[16] Within this family, the rhodate, $Cu_{1-x}Ag_xRh_{1-y}Mg_yO_2$ has been recently investigated as a potential thermoelectric material.[17] The structure (Fig. 1) has $CoO_2$ sheets similar to $Na_xCoO_2$, but these are connected quite differently perpendicular to the layers. In particular, $Na_xCoO_2$ has $CoO_2$ sheets separated by a Na layer with partially filled sites, while the sheets in $CuCoO_2$ are joined by Cu atoms, which form bridges between O ions in the adjacent sheets. This provides a three dimensionally connected structure that may be more isotropic from an electronic point of view as well.

The calculations were done in the local density approximation (LDA) using the general potential linearized augmented plane wave (LAWP) method,[18] as implemented in two codes, which were cross-checked. These were an in-house code and the WIEN2K code.[19] Local orbitals[20] were used to relax the linearization of the *d* bands and to accurately treat the semicore states of Cu and Co as well as the O 2*s* state. The calculations of the thermopower were per-

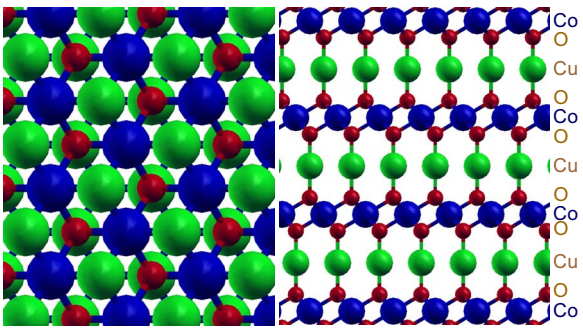


FIG. 1. (Color online) Crystal structure of $CuCoO_2$. Co is shown as dark blue spheres, Cu as light green, and O as small dark red spheres. The left panel shows a view along the *c* axis, while the right panel has the *c* axis in the vertical direction. The rhombohedral unit cell contains 1 f.u.

 

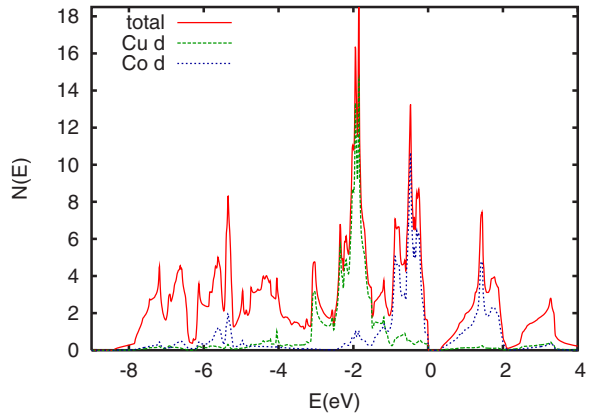


FIG. 2. (Color online) LDA density of states and Cu and Co $d$ projections onto LAPW spheres for $CuCoO_2$. The LAPW sphere radius for the projections was $1.90a_0$ for both Cu and Co. The energy zero is set at the valence band maximum.

formed using the BOLTZTRAP code,[22] applied as in Ref. 14. A $32^3$ set of **k** points was used for the zone sampling in the transport calculations. This yielded converged results above 200 K for the doping levels considered here. The experimental lattice parameters, $a=2.849$ Å and $c=17.141$ Å,[15] as determined by diffraction, were used. The internal parameter, corresponding to the O height above the triangular lattice Co planes may be of importance.[21] The calculations shown were done using the value $z_O=0.109\,74$, which was obtained from LDA total energy minimization. This value is quite close to the reported experimental value, $z_O=0.111$.[15] The calculated value of the corresponding full symmetry Raman frequency was $\omega(A_g)=616\ \mathrm{cm}^{-1}$.

Figures 2 and 3 show the calculated electronic density of states and projections onto the LAPW spheres and the band structure, respectively. Although, as mentioned, the calculations were done using the rhombohedral primitive cell, the bands are plotted in a hexagonal extended zone scheme to facilitate comparison with $Na_xCoO_2$ and to show in-plane and out-of-plane directions.

As may be seen, the Cu $d$ states are located in the energy range from approximately −3 to −1.5 eV with respect to the valence band edge. Therefore, Cu occurs as $Cu^{1+}$ in this material. This means that the Co is nominally $Co^{3+}$, with six $d$ electrons, and that the Fermi energy occurs between the occupied $t_{2g}$ and unoccupied $e_g$ manifolds. The widths of these manifolds are very narrow as in $Na_xCoO_2$ and related layered rhodates. However, as may be seen in Fig. 3, higher lying, free-electron-like bands disperse downward into the $e_g$ manifold at some places in the zone and mix with the $e_g$ states at the bottom of the conduction band manifold. This leads to dispersions around the conduction band edge with lighter masses that would be anticipated from the narrow $e_g$ bandwidth. The band structure is not nearly as two dimensional as $Na_xCoO_2$. For hole doping in the range 0.05–0.25/unit cell, the ratio of the in-plane to out-of-plane low temperature $\sigma/\tau=N(E_F)\ \langle v_F^2\rangle$ varies between 1.5 (high doping) and 3.5 (low doping), while for $n$-type doping the range is from 0.7 to 0.9. Here, $\sigma$ is the conductivity as obtained from Boltzmann kinetic transport theory,[9,11,12,22] $\tau$ is the scattering time, $\langle v_F^2\rangle$ is the average of the squared Fermi velocity in the direction of interest, and $N(E_F)$ is the density of states at the Fermi energy. While the scattering time may be anisotropic, these small ratios imply that from a transport point of view the material is quite three dimensional and, in fact, that for $n$-type doping the high conductivity direction may be perpendicular to the $CoO_2$ sheets.

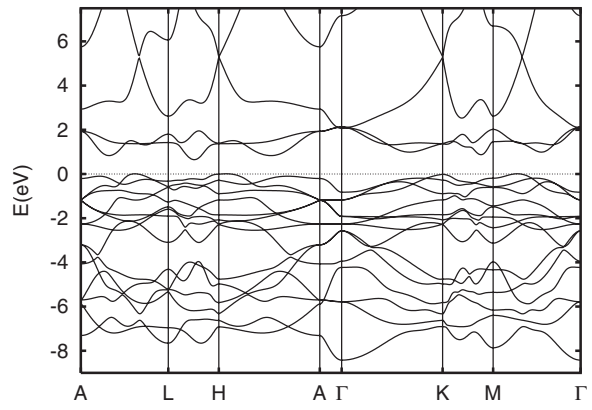


FIG. 3. LDA band structure (top) of rhombohedral $CuCoO_2$ in an extended hexagonal zone scheme.

Another significant difference from the electronic structure of $Na_xCoO_2$ and related rhodates is that the calculated $CuCoO_2$ band gap of 0.38 eV between the $t_{2g}$ and $e_g$ manifolds is much smaller than the corresponding gaps in those compounds. While it is well known that in most materials LDA band structure calculations underestimate band gaps, this does not apply to crystal field gaps, where LDA predictions are often similar to experiment.[23,24] The implication is that achieving $n$-type doping is much more likely in $CuCoO_2$ than in $Na_xCoO_2$.

Within the standard Boltzmann kinetic transport theory, the thermopower is given by[8,9]

$$S_{\alpha\beta}=\sum_{\gamma}(\sigma^{-1})_{\alpha\gamma}\nu_{\gamma\beta}, \tag{1}$$

where

$$\sigma_{\alpha\beta}(T,\mu)=\frac{1}{\Omega}\int\sigma_{\alpha\beta}(\epsilon)\left[-\frac{\partial f_\mu(T,\epsilon)}{\partial\epsilon}\right]d\epsilon, \tag{2}$$

$$\nu_{\alpha\beta}(T,\mu)=\frac{1}{eT\Omega}\int\sigma_{\alpha\beta}(\epsilon)(\epsilon-\mu)\left[-\frac{\partial f_\mu(T,\epsilon)}{\partial\epsilon}\right]d\epsilon, \tag{3}$$

and

$$\sigma_{\alpha\beta}(\epsilon)=e^2\int d^3\mathbf{k}\,\tau(\mathbf{k})v_\alpha(\mathbf{k})v_\beta(\mathbf{k})\delta[\epsilon-\epsilon(\mathbf{k})]. \tag{4}$$

The $\epsilon(\mathbf{k})$ are the band energies, $v_\alpha(\mathbf{k})$ are the band velocities, $\partial\epsilon(\mathbf{k})/\partial k_\alpha$, $\tau(\mathbf{k})$ is the scattering time, $\mu$ is the chemical potential, and $f_\mu$ is the Fermi function.

The so-called constant scattering time approximation is common for degenerately doped semiconductors and metals. In this case, the scattering time keeps its full, and normally strong, temperature and doping level dependence, but it is

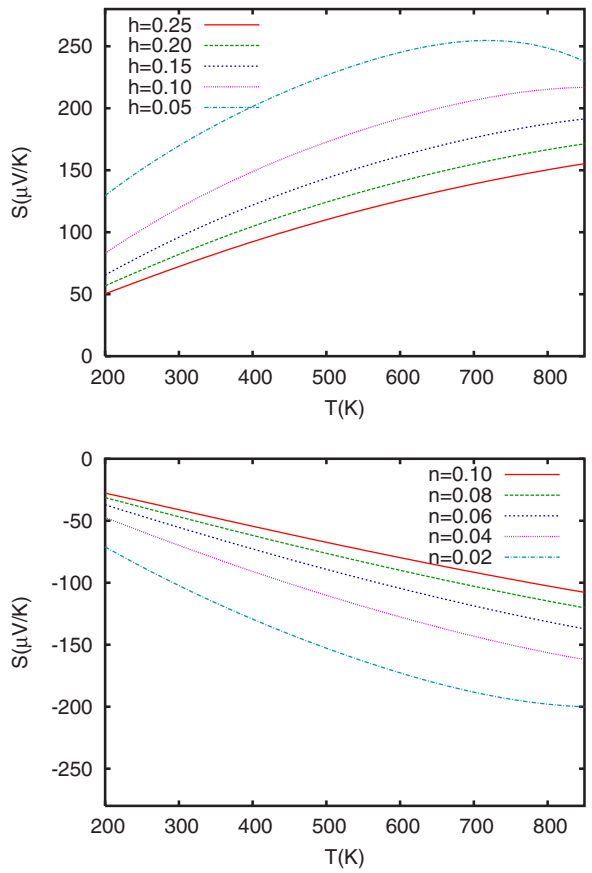


FIG. 4. (Color online) Calculated in-plane thermopower as a function of temperature using the constant scattering time approximation. The top panel is for hole doped $CuCoO_2$ and the bottom panel is for electron doping. Carrier densities $n$ and $h$ are given in carriers per f.u. Note that different carrier densities are shown for $p$ type and $n$ type.

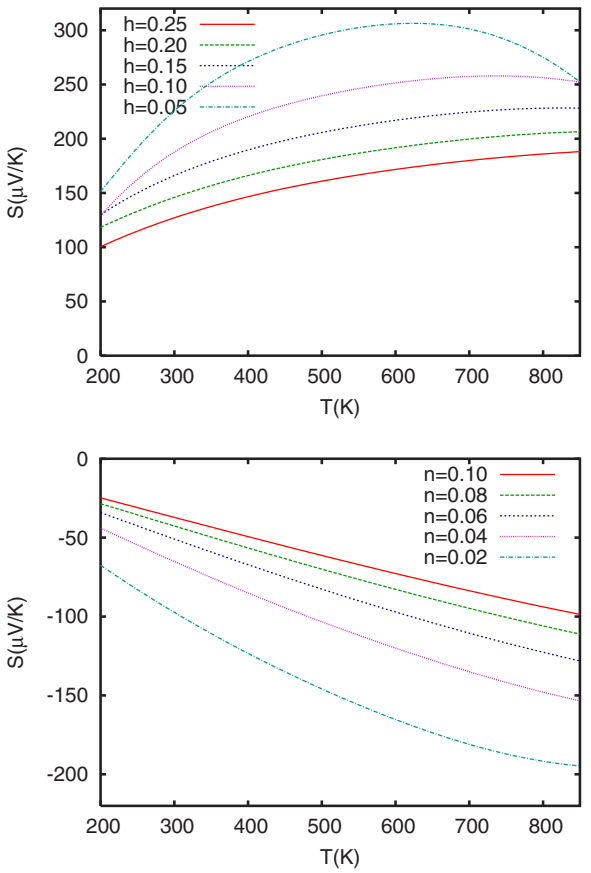


FIG. 5. (Color online) Calculated $c$-axis thermopower as a function of temperature using the constant scattering time approximation, as in Fig. 4. $CuCoO_2$ and the bottom panel are for electron doping.

assumed that $\tau$ is energy independent at fixed doping and temperature. This approximation, applied to $Na_xCoO_2$, yields a quantitative agreement with experiment for the thermopower.[11,12] The advantage of using this approximation is that it does not require knowledge of the detailed scattering mechanisms, which may be dependent on sample preparation, and that when it is made the scattering time cancels in the expression for $S(T)$. Therefore, one obtains a quantitative prediction for $S(T)$ directly from the band structure with no adjustable parameters.

In the calculations shown here, we imposed a fixed net carrier concentration, defined as the number of electrons minus the number of holes. This is appropriate for the case where the material is doped by chemical means. The function $\mu(n,T)$ was calculated and used to obtain $S(n,T)$ from the calculated $S(\mu,T)$. Both conduction and valence bands were included in the calculations. This leads to a decrease in the magnitude of the thermopower at high temperature and low doping level due to the contribution of thermally populated opposite sign carriers.

Figures 4 and 5 show the calculated $S(T)$ for $p$- and $n$-type doping for the in-plane and out-of-plane directions respectively. As may be seen, the in-plane thermopower is quite similar to that of $Na_xCoO_2$ for $p$-type doping, except that at low doping the thermopower decreases at high temperature. This is a consequence of the lower band gap. This is in spite of the fact that the detailed band dispersion near the valence band edge is rather different from that of $Na_xCoO_2$, a fact that underscores the result that the key to the high thermopower is the narrowness of the $t_{2g}$ manifold and not the detailed distribution of the carriers in the different suborbitals. Perhaps of more significance is the out-of-plane thermopower, which is also high and positive. This is different from that of $Na_xCoO_2$. Recalling the three dimensional transport expected based on the calculated $\sigma/\tau$, the implication is that if $CuCoO_2$ can be doped with mobile holes, its thermoelectric performance in ceramic form may be more similar to that of oriented crystals than is the case in $Na_xCoO_2$.

Turning to $n$-type dopings, the thermopower at fixed carrier concentration is lower than that for $p$-type doping, both in plane and out of plane. This is due to the greater dispersion at the conduction band edge, which results from the free electron bands that, as mentioned above, enter the Co $e_g$ manifold. However, quite high values of the thermopower can be obtained in the temperature range of interest for waste heat recovery if smaller, but still high, doping levels of $\sim 0.05-0.10$ electrons per Co are used. In the case of $n$-type

doping, the anisotropy of the thermopower tensor is small, as is the anisotropy of the conductivity, as measured by that of $\sigma/\tau$.

Therefore, $CuCoO_2$ has a potential to be a good thermoelectric material for waste heat recovery if it can be doped with mobile charge carriers. This is based on the calculated thermopowers using the LDA band structure as input. It depends on having carrier mobilities and lattice thermal conductivities comparable to those of $Na_xCoO_2$. We note that it is not known if mobile carriers can exist in $CuCoO_2$, nor is it known what the lattice thermal conductivity will be in such samples. Nonetheless, based on the similarity of the structure and chemistry of the $CoO_2$ sheets in $CuCoO_2$ to those in $Na_xCoO_2$, it is not unreasonable to suppose that the thermal conductivity could be similar to the value in that material. If so, the present results regarding the thermopower indicate that $CuCoO_2$ would be a good thermoelectric both for *n*-type and *p*-type doping. From a more fundamental point of view, $CuCoO_2$ represents a material that is related to $Na_xCoO_2$ in terms of the similar $CoO_2$ sheets in the two materials but is quite three dimensional in contrast to the two dimensional electronic structure of $Na_xCoO_2$. In both compounds, high thermopowers are found in band structure calculations, which do not include Hubbard correlations beyond the LDA level. Measurements of thermopower in comparison with the present results may shed light on the role of correlations in the cobaltates.

This work was supported by the Freedom Car and Vehicle Technologies Program of the EERE, Department of Energy. I am grateful for helpful discussions with D. G. Mandrus. Figure 1 was produced using the XCRYSDEN program (Ref. 25).

[1] The thermoelectric figure of merit is $ZT=\sigma S^2 T/\kappa$, where $\sigma$ is the electrical conductivity, $S$ is the thermopower, and $\kappa$ is the thermal conductivity, including both the electronic and lattice contributions.

[2] I. Terasaki, Y. Sasago, and K. Uchinokura, Phys. Rev. B **56**, R12685 (1997).

[3] K. Fujita, T. Mochida, and K. Nakamura, Jpn. J. Appl. Phys., Part 1 **40**, 4644 (2001).

[4] H. Liligny, D. Grebille, O. Perez, A. C. Masset, M. Hervieu, C. Michel, and B. Raveau, C.R. Acad. Sci., Ser. IIc: Chim **2**, 409 (1999).

[5] S. Hebert, S. Lambert, D. Pelloquin, and A. Maignan, Phys. Rev. B **64**, 172101 (2001).

[6] Y. Miyazaki, M. Onoda, T. Oku, K. Kikuchi, Y. Ishii, Y. Ono, Y. Morii, and T. Kajitani, J. Phys. Soc. Jpn. **71**, 491 (2002).

[7] W. Koshibae, K. Tsutsui, and S. Maekawa, Phys. Rev. B **62**, 6869 (2000).

[8] W. Jones and N. H. March, *Theoretical Solid State Physics* (Dover, New York, 1985).

[9] J. M. Ziman, *Principles of the Theory of Solids* (Cambridge University Press, Cambridge, 1972).

[10] D. J. Singh, Phys. Rev. B **61**, 13397 (2000).

[11] H. J. Xiang and D. J. Singh, report, 2007 (unpublished).

[12] D. J. Singh and D. Kasinathan, J. Electron. Mater. **36**, 736 (2007).

[13] D. J. Singh, *Semicondcutors and Semimetals*, Thermoelectric Materials Research Vol. 70 (Academic, New York, 2000), p. 125.

[14] G. B. Wilson-Short, D. J. Singh, M. Fornari, and M. Suewattana, Phys. Rev. B **75**, 035121 (2007).

[15] E. F. Bertaut and C. Delorme, Acad. Sci., Paris, C. R. **238**, 1829 (1954).

[16] E. F. Bertaut and J. Dulac, J. Phys. Chem. Solids **21**, 118 (1961).

[17] S. Shibasaki, W. Kobayashi, and I. Terasaki, Phys. Rev. B **74**, 235110 (2006).

[18] D. J. Singh and L. Nordstrom, *Planewaves Pseudopotentials and the LAPW Method*, 2nd ed. (Springer, Berlin, 2006).

[19] P. Blaha, K. Schwarz, G. K. H. Madsen, D. Kvasnicka, and J. Luitz, *WIEN2K: An Augmented Plane Wave + Local Orbitals Program for Calculating Crystal Properties* (K. Schwarz, TU Wien, Austria, 2001).

[20] D. Singh, Phys. Rev. B **43**, 6388 (1991).

[21] The Co ions in $CuCoO_2$ and $Na_xCoO_2$ occur on a site with rhombohedral symmetry. This leads to a splitting of the $t_{2g}$ orbitals into an $a_g$ state, directed along the *c* axis, and two $e_g'$ states. The relative energy of these two states is important in the band formation and is strongly affected by the O height.

[22] G. K. H. Madsen and D. J. Singh, Comput. Phys. Commun. **175**, 67 (2006).

[23] L. F. Mattheiss, Phys. Rev. B **43**, 1863 (1991).

[24] D. J. Singh, R. C. Rai, J. L. Musfeldt, S. Auluck, N. Singh, P. Khalifah, S. McClure, and D. G. Mandrus, Chem. Mater. **18**, 2696 (2006).

[25] A. Kokalj, J. Mol. Graphics Modell. **17**, 176 (1999); code from http://www.xcrysden.org